Feasibility study of energy storage by concentrating/desalinating water: Concentrated Water Energy Storage

Wei He [a, *] and Jihong Wang [a, b]

[a] School of Engineering, University of Warwick, Coventry, United Kingdom

[b] School of Electrical & Electronic Engineering, Huazhong University of Science & Technology, China

Abstract:

The paper is to report the work on a preliminary feasibility study of energy storage by concentrating/desalinating water. First, a novel concentrated water energy storage (CWES) is proposed which aims to use off-peak electricity to build the osmotic potential between water bodies with different concentrations, namely brine and freshwater. During peak time, the osmotic potential energy is released to generate electricity.

Two scenarios of CWES are specified including a CWES system using reverse osmosis (RO) and pressure retarded osmosis (PRO), and a CWES system co-storing/generating energy and freshwater using "osmotic-equivalent" wastewater. A comprehensive case study is carried out with focusing on the configuration of CWES using RO and PRO. It is found that the limiting cycle efficiency of the CWES using RO and PRO is inversely proportional to the RO water recovery and independent of the initial salinity. Therefore, to balance the energy density and cycle efficiency of CWES, it is recommended to operate a system at lower RO water recovery with higher concentration of the initial solution. Detailed energy analysis of detrimental effects in mass transfer, e.g. concentration polarization and salt leakage, and energy losses of pressurisation and expansion of pressurised water, are studied. Finally, a preliminary cost analysis of CWES is given.

Keywords:

Concentrated Water Energy Storage, Osmotic Energy, Water Desalination, Pressure Retarded Osmosis, Reverse Osmosis

1. Introduction

Rapidly increase of the power generation from renewable energy sources has been achieved to reduce the usage of fossil fuels and the emissions of carbon dioxide [1]. By the year's end of 2014, renewables, mainly including the wind, solar PV and hydropower, account for an estimated 27.7% of the world's power generation capacity, enough to supply an estimated 22.8% of global electricity [2]. However, due to the unavoidable intermittence of the most renewable energy sources, there exists a great challenge in the power generation and load balance maintenance to ensure the stability and reliability of the power network. Electrical energy storage normally presents a process to convert electricity from grid or renewables into a form that can be stored for releasing back to generate electricity when needed. It provides the power management as an energy buffer to dispatch electrical energy in a flexible way [3]. With sufficient energy storage capacity, the total power generation capacity can be built to meet average electricity demand rather than peak demands [4]. Until now,

* Corresponding author: Tel: + 44(0)20 7882 3774(W He)
E-mail address: w.he.1@warwick.ac.uk

there are mainly two commercialised bulk energy storage technologies, namely pumped hydroelectric storage (PHS) [5, 6] and compressed air energy storage (CAES) [7]. As reported by the Electric Power Research Institute, PHS presents more than 99% of bulk energy storage capacity in the world and about 3% of global electricity generation, approximately an installed 127 GW in 2012 [8-10]. For CAES, there are two CAES plants in operation. The first utility-scale CAES project is the 290 MW Huntorf plant in Germany using the salt dome for storage, which was built in 1978. The other is an 110 MW plant with a capacity of 26 hours in McIntosh, Alabama.

However, current commercialised large-scale energy storage technologies are subject to geographic restrictions. A site for a PHS plant must be suitable for the construction of standing or dammed-up water reservoirs, and the capacity of the reservoir [11]. For building large-scale CAES plants, concerning the storage capacities up to several hundreds of megawatts, underground salt caverns, natural aquifers, and depleted natural gas reservoirs are potentially the most appropriate options [9]. The dependence on these specific geographic sites restricts the deployment of the large-scale energy storage systems of both PHS and CAES. In fact, installation of new PHS plants inclined since 90's due to the environmental concerns and scarcity of favourable sites [12] and the potential for the further major PHS schemes would also be restricted [13]. Also, excluding storing the compressed air underground, it is challenge for CAES plants storing the compressed air above the ground to have bulk scale[14]. So the paper is to explore an alternative way for implementation of bulk energy storage.

In this study, feasibility study of an innovative bulk energy storage by concentrating/desalinating water is conducted by employing technologies of desalination and osmotic energy generation. Since the mid-20th century desalination has been demonstrated to be a viable approach to broaden the current drinkable water supplies and has been widely and successfully used to produce freshwater in the Middle East and North African countries [15]. In addition, generation of osmotic energy, or salinity energy, from salinity gradients has been identified as a promising technology [16]. Similar to the reverse processes of lifting and releasing of water head in PHS, and processes of compressing and expanding air in CAES, desalination and osmotic energy generation are reverse processes to concentrate/desalinate and mix saline waters. Electricity is used to desalinate freshwater from saline stream to overcome the increased concentration difference. During mixture of the two streams, electricity is generated from the chemical potential between salinity gradients. Therefore, these two processes theoretically can be integrated to fulfil a cycle of charge and discharge to store electricity during off-peak and generate power during peak time. Moreover, compared to PHS and CAES, a significant advantage of desalination and osmotic energy generation is that freshwater can be produced with energy storage. It allows potential co-generation (or co-storage) of energy and freshwater in the hybrid system simultaneously. Additionally, the salinities can be stored in ambient temperature/pressure/height without geometric restrictions of CAES or PHS. Therefore, taking these potential advantages and the significant improvements on the osmotic energy generation technologies, a question arises: how about the performance of this new energy storage system ?

The answer has not been found from the published studies yet. Only limited investigations focusing on a prototype using osmotic energy generator in thermal energy conversion have been envisioned. A process based on a closed-loop pressure retarded osmosis (PRO) has been recently proposed as an approach of transforming unusable low-grade thermal energy, such as waste heat, into electricity to the power network [17]. The process, also called an osmotic heat engine, enables a form of osmotic grid storage for available thermal energy and intermittent renewables [17-19]. It was estimated to be ~ 1kWh/m^3 energy density of an osmotic battery at the hypothetical operating limit of 80 bar PRO module [20]. However, all these investigations are concentrated on the performance of the membrane or/and the evaluation of different draw solutions. There is a lack of comprehensive analysis at the system level to address the overall efficiency of the whole system as an energy storage

technology. To analyse an energy storage technology, it mainly includes energy density, cycle efficiency (or round-trip efficiency), cycling times, self-discharge rate and etc. [10]. Therefore, it calls for a preliminary study to evaluate the overall performance of the combined desalination and osmotic energy generator.

Therefore, feasibility study of the new bulk energy storage using desalination and osmotic energy generator is carried out in this work to fill the knowledge gap. In this study, a proposed system called concentrated water energy storage (CWES) which can be used as a large-scale energy storage system is introduced at first. A generic CWES system is introduced and the energy density of the stored water is analysed in Section 2. Then, several scenarios of the CWES are discussed and configured in Section 3. In Section 4, a case study of the CWES using reverse osmosis (RO) and PRO is systematically carried out.

2. Concentrated water energy storage

2.1. Technologies of desalination and osmotic energy generation

At present, desalination plants are operated worldwide to produce freshwater at a rapidly increasing rate. From 2007 to 2015, the total installed desalination capacity has increased from 47.6 million cubic meters per day to approximated 97.5 million cubic meters per day [21, 22]. For a plant, the single largest seawater desalination plant is Ras AI-Khair in Saudi Aravia which produces 1.025 million cubic meters per day in 2014 [23], and it will be surpassed by a desalination plant in California in near future [24]. The enormous amount of desalination capacity demonstrates the capability of the technologies to be scaled up, which also validates the possibility of storing the bulk energy in terms of salinity gradients through the current desalination facilities.

Desalination can be mainly classified into two categories including thermal-driven desalination and electricity-driven desalination. Traditional thermal-driven desalination approaches include multi-stage flash (MSF) [25], multi-effect distillation (MED) [26] and thermal vapour compression (TVC) [27]. Recently, several novel approaches are proposed and investigated to enrich the portfolio of the thermal-driven desalination, in which adsorption desalination (AD) [28], membrane distillation (MD) [29], forward osmosis (FO) with thermally recovering draw solution [30], and humidification-dehumidification (HDH) [31] emerge rapidly. Comprehensive reviews and comparisons of these technologies can be found in [15, 32]. In addition to thermally-driven approaches, major electricity-driven desalination plant consists of reverse osmosis (RO) [33], electrodialysis (ED) [34], mechanical vapour compression (MVC) [35] and capacitive deionization (CDI) [36]. Among these desalination approaches, RO is the most utilised electricity-driven desalination technology. While MSF and MED are the ones used most widely thermal-driven processes. In 2009, RO accounts for 59% of installed capacity of desalination, followed by MSF at 27% and MED at 9% [37].

Approaches to extract osmotic energy have been widely investigated in last decade. Well-developed techniques to generate the osmotic energy includes PRO [38], reverse electrodialysis (RED) [39], and several emerging approaches, such as capacitive mixing (CAPMIX) [40], and Faradaic pseudo-capacitor [41]. A brief review of the current technologies to recover the osmotic energy can be found in [42]. Currently, the most explored technologies of the osmotic energy generators are PRO and RED. PRO can be regarded as an “osmotic-assist” hydro-electric technology. In a PRO osmotic power plant, two saline streams with different salinities flow at the two sides of a semi-permeable membrane. Naturally, due to the non-zero solute difference across the membrane, the water permeates from the feed (low concentration solution) side to the draw (high concentration solution) side. Applying a hydraulic pressure that is lower than the initial osmotic pressure difference between the two salinities on the draw solution, because of the osmosis phenomenon, the chemical potential between the two salinity gradients is converted into the hydro-electric potential of the permeation. Thus, by controlling the applied pressure and flow rates of the salinity gradients, the osmotic energy generated from a

PRO plant is harvested by expanding the pressurised permeation in a hydro-turbine [43]. In 2009, the world's first osmotic power plant using PRO was launched in Norway with a 4kW capacity [38]. In Japan, a project called "Mega-ton Water System" aims to develop an energy efficient and chemical-free dual purpose plant with 1 mega-ton per day desalination capacity (1 million m^3, equivalent to the daily needs of approximately 4 million people) and 100,000 m^3 per day sewage wastewater reclamation by PRO using concentrated brine from seawater desalination and treated sewage [44]. According to their prototype plant test conducted in Japan using brine from seawater desalination and freshwater from regional wastewater treatment, the maximum membrane power density is as high as 13.5 W/m^2 using 10-in module [45], which is higher than the estimated membrane performance to achieve the economic viability (5 W/m^2 estimated by Gerstandt et al. [46]). Recently, a demonstration membrane distillation (MD) and PRO hybrid desalination demonstration plant started to be built in Korea [47]. Additionally, RED is the reverse process of electrodialysis in desalination. In a RED, seawater and freshwater are pumped into arrays or stacks with alternating selective membranes. Due to the concentration difference of solutions and ion-selectivity of the membranes, the electric potential is generated and controlled. The potential is a result of the determined flow direction of the ions in seawater. The first RED system in the world generating electricity from brine is now operating, which has been installed and operated by the University of Palermo [48].

2.2. Schematic diagram of a CWES

A generic CWES which is a hybrid system of a desalination plant and an osmotic power plant is shown in Fig. 1. Current osmotic energy generations commonly use natural salinities such as seawater, brackish water and river water to generate electricity. In contrast, CWES pre-concentrates the initial saline stream using low-cost electricity from the power grid at off-peak time, and utilises it to generate electricity when required. During the charge period, the off-peak electricity is converted into chemical potential between the two salinities via the separation process, namely concentrated stream (brine reservoir) and dilute stream (permeate reservoir).

CWES has two apparent advantages: on one hand, saline streams can be stored in appropriate tanks or reservoirs at ambient temperature and pressure at any height without geological conditions restricted by either PHS or CAES. On the other hand, CWES benefits both sub-systems of desalination and osmotic energy generation, which include efficient freshwater production, reclamation of the concentrated water from desalination and significant increase of the membrane power density in osmotic energy generation.

In addition, the proposed CWES has many similarities to the current bulk energy storage systems. In a CWES, during the charge period, concentrating water by pumps is similar to compressing air by compressors in a CAES. During the discharge period, the osmotic potential is converted into hydro-electric potential and produce electricity in hydro-turbines, which is similar to the discharge process of PHS. Consequently, the proposed CWES can be regarded as a combination of a CAES and a PHS, a system of pumped osmotic-hydro-electric storage by changing concentration. The novel energy storage system inherits the features of the current two bulk energy storage systems, namely very low self-discharge, easy scale-up, low cost and tolerance of hostile environment. Moreover, CWES is capable to potentially take advantages of the previous experiences in system design and development of components in PHS, such as high pressure water pumps and hydro-turbines.

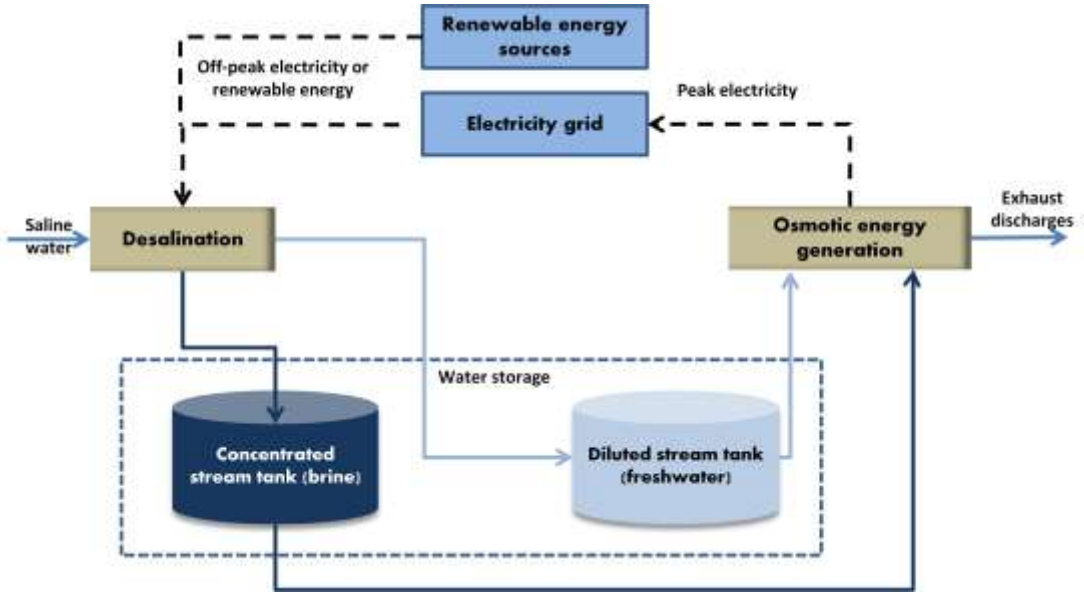

Figure 1 Schematic diagram of a generic CWES system.

2.3. Thermodynamic limits of a CWES and energy density of stored water

Several comprehensive reviews on the different energy storage approaches can be found in [3, 10, 49, 50]. According to [3], current large scale energy storage, such as CAES and PHS, the stored energy density is about 0.5 – 1.5 Wh/L for PHS and 3-6 Wh/L for CAES. Before design and analysis of the configuration of the proposed CWES, in this section, the maximum energy density of a generic CWES can be evaluated by carrying out a thermodynamic analysis based on the Gibbs free energy of mixing.

The Gibbs free energy of mixing is released when solutions with different salinity concentrations are combined. The maximum energy to be potentially harvested between the mixing of the two salinities can be determined by the reversible thermodynamic analysis. Therefore, the energy stored in two salinity reservoirs can be evaluated by the Gibbs free energy of mixing, which is [51],

$$-\Delta G_{MIX} = RT\{[\sum x_i \ln(\gamma_i x_i)]_M - \phi_{high}[\sum x_i \ln(\gamma_i x_i)]_{high} - \phi_{low}[\sum x_i \ln(\gamma_i x_i)]_{low}\} \quad (1)$$

where x_i the mole fraction of species i in solution, R is the gas constant, T is temperature, γ_i is activity coefficient which is incorporated to present the non-ideal solutions. ϕ_{high} and ϕ_{low} are the ratios of the total moles in solution with high concentration and low concentration, respectively.

Lin et al. simplified the expression of the Gibbs free energy and derived an approximation of the specific Gibbs free energy of mixing per volume of total mixed solution [52]. It is represented as

$$-\Delta G_{MIX,V_M} = \nu RT[c_M \ln(c_M) - \phi c_{low} \ln(c_{low}) - (1-\phi) c_{high} \ln(c_{high})] \quad (2)$$

where ν is the van't Hoff factor for strong electrolyte and ϕ is the dimensionless flow rate which is the ratio of the low concentration solution flow rate to the sum of flow rates of both solutions.

Because of the nature of incompressibility of the water, the volume of the total mixed solution is the sum of the volumes of the high concentrated and low concentrated solutions. Consequently, based on equation (2), the specific Gibbs free energy per volume of the total mixed solution can be used to evaluate the energy density of the generic CWES as shown in Fig. 1. For a generic desalination plant as shown in Fig. 1, part of the pure water is separated from the saline water. Simultaneously, concentrated brine is resulted. A concept of water recovery is defined as the ratio of the produced

freshwater's mass flow rate to that of the initial saline water. In an ideal separation with no salt leakage, based on the mass balance of the solute and water as represented below,

$$c_S q_S = c_B q_B + c_P q_P; \quad q_S == q_P + q_P; \tag{3}$$

where c and q are concentration and mass flow rate, and subscripts, s, b and p, represent the saline water, brine and permeation from the desalination. Due to c_P is considerably smaller than c_B, concentration and flow rates of the brine can be approximately expressed as,

$$c_B = \frac{c_S}{1-Y}; q_B = q_S(1-Y); \tag{4}$$

where Y is water recovery ratio which is q_P / q_S.

On the basis of the models derived above, energy density of a generic CWES system as shown in Fig. 1 can be evaluated. The estimated energy densities of the CWES with respect to different water recovery ratios are shown in Fig. 2 in which freshwater concentration is assumed to be 0.01 g/L. According to the results, the theoretical maximum energy density of a generic CWES using seawater as the initial saline stream is close to 1.5 Wh/L for the energy storage. For the purposes of comparisons, the theoretical maximum energy densities of PHS and CAES are also estimated based on thermodynamic analysis (detailed derivation and calculation can be found in Appendix). The results of energy densities of PHS and CAES are shown in Fig. 2(b) and 2(c), respectively. The range of the energy density of a CWES in energy storage is close to those of PHS. In addition, if the concentration of the initial saline stream is increased, the resulted energy density of the stored water is also enhanced. As shown in Fig. 2(a), the energy density of the stored water can be more than 2.5 Wh/L when the concentration of the initial saline stream is approximately 70 g/L.

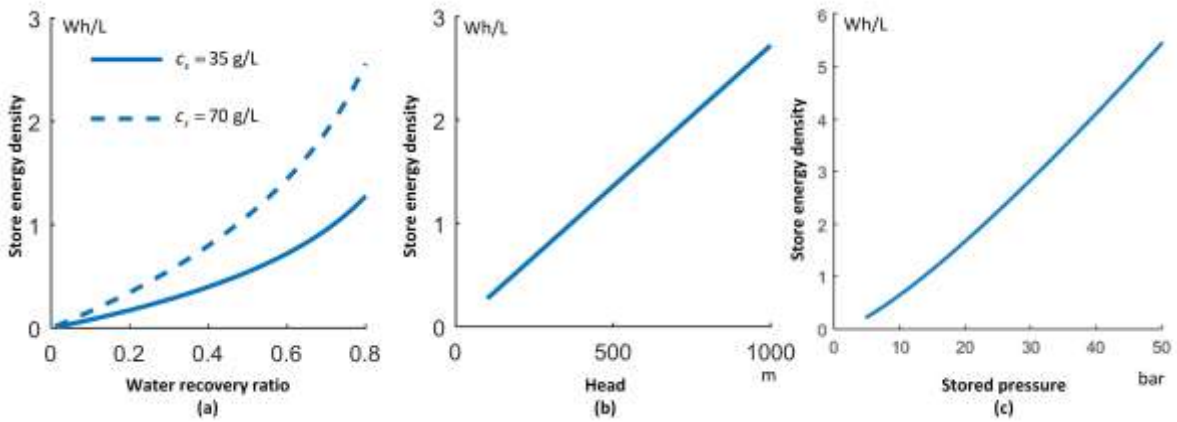

Figure 2 Maximum store energy densities of the generic CWES with respect water recovery ration in (a), maximum energy densities of PHS with pressure head in (b), and maximum energy densities of CAES with respect to stored pressure of compressed air in (c).

3. Two scenarios of CWES system

CWES shown in Fig. 1 is a generic schematic configuration. In fact, a number of approaches can be found in both desalination and osmotic energy generation and a number of combinations are capable

to be selected and studied. In this section, two configurations of CWES using RO and PRO are specified at the early stage.

3.1. CWES using RO and PRO

To be functioned as electrical energy storage, CWES using RO as the electricity-driven desalination and PRO as osmotic energy generator is promising because of: 1) ease of using electricity from the grid during the off-peak time to drive RO desalination plant; 2) mature technology of RO and rapid development of PRO. A schematic CWES using RO and PRO is shown in Fig. 3. The CWES can be divided into three sub-systems: desalination sub-system, water storage sub-system and osmotic energy generator sub-system. During the charge time of low power demand, in desalination sub-system, seawater is pressurized by energy recovery device (ERD) and high-pressure pump (HP) before flowing into the RO membrane module. Due to the separation of RO, concentrated brine and diluted freshwater are produced, flowing into the water storage sub-system. They are stored in different tanks/reservoirs, respectively. At the discharge period in the high power demand, the stored salinities gradients are pumped into osmotic energy generator using boost pump (BP). The concentrated brine is pressurized by HP and ERD before flowing into membrane module. Due to the permeation inside of the PRO membrane module, the chemical potential is converted into hydro-electric energy and harvested in the hydro turbine (HT) and connected to grid.

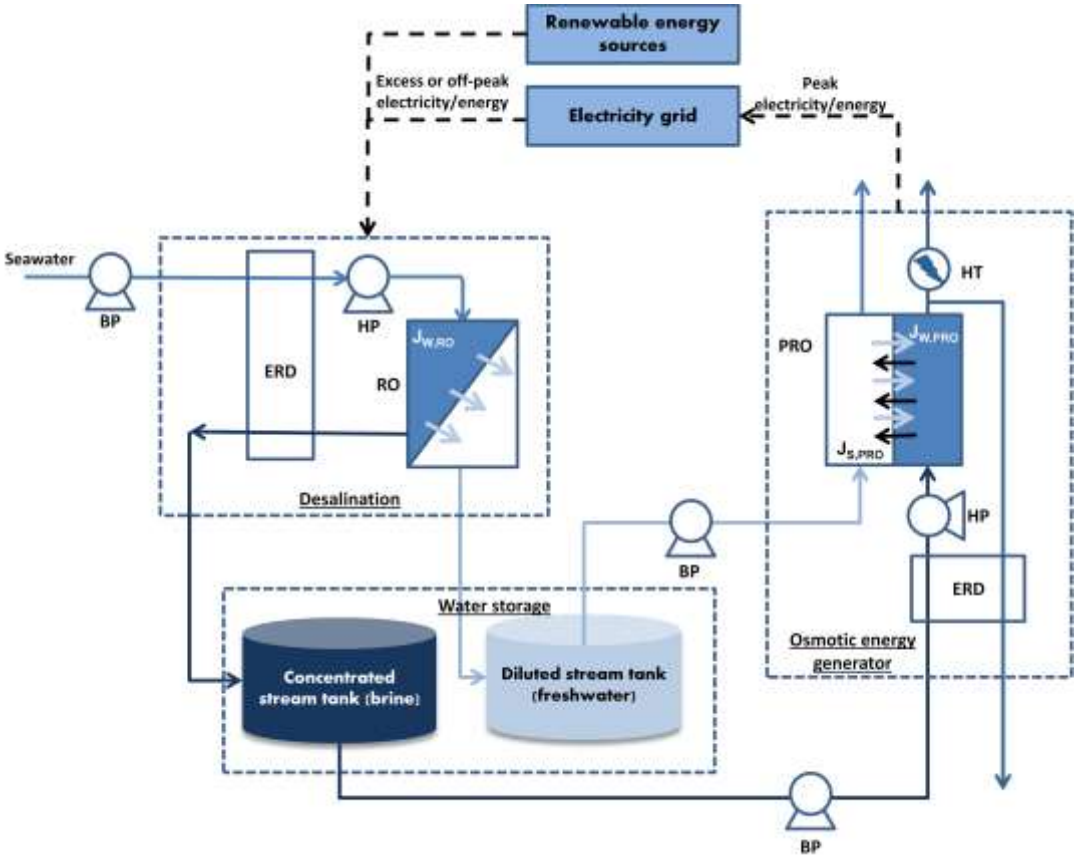

Figure 3 Schematic illustration of CWES using RO and PRO.

3.2. CWES using "osmotic-equivalent" reclaimed wastewater

Compared to energy/electricity, freshwater is also a scarce resource. In the proposed CWES systems, produced dilute stream as an energy carrier is stored in the storage system. Actually, the quality of the produced water from RO desalination is potentially high enough for drinking or

irrigating. Therefore, freshwater is also a product. A configuration of the CWES using reclaimed wastewater is shown in Fig. 4. In the system, the "osmotic equivalent" reclaimed wastewater is used to replace the freshwater as the dilute solution flowing into the osmotic energy generation sub-system. Because of the negligible difference between the concentrations of the freshwater and the wastewater, the performance of the PRO will not be significantly changed if membrane fouling is controlled. But the fouling propensity of the membrane using reclaimed wastewater would be enhanced. In order to prolong the lifetime of the membrane and maintain the system performance, reclamation of the wastewater for the PRO osmotic energy generator need to be pre-treated. In this case, the CWES coupled with freshwater production also increases the potential economic viability of the whole system. Excluding the electricity demands, the operation of CWES is possibly further considered based on the peak and off-peak water consumption in the high and low demand. Selling freshwater and recovering/reusing wastewater are able to improve the economic viability of the proposed CWES, but it calls for detailed optimization in operations of storage and production of water and energy.

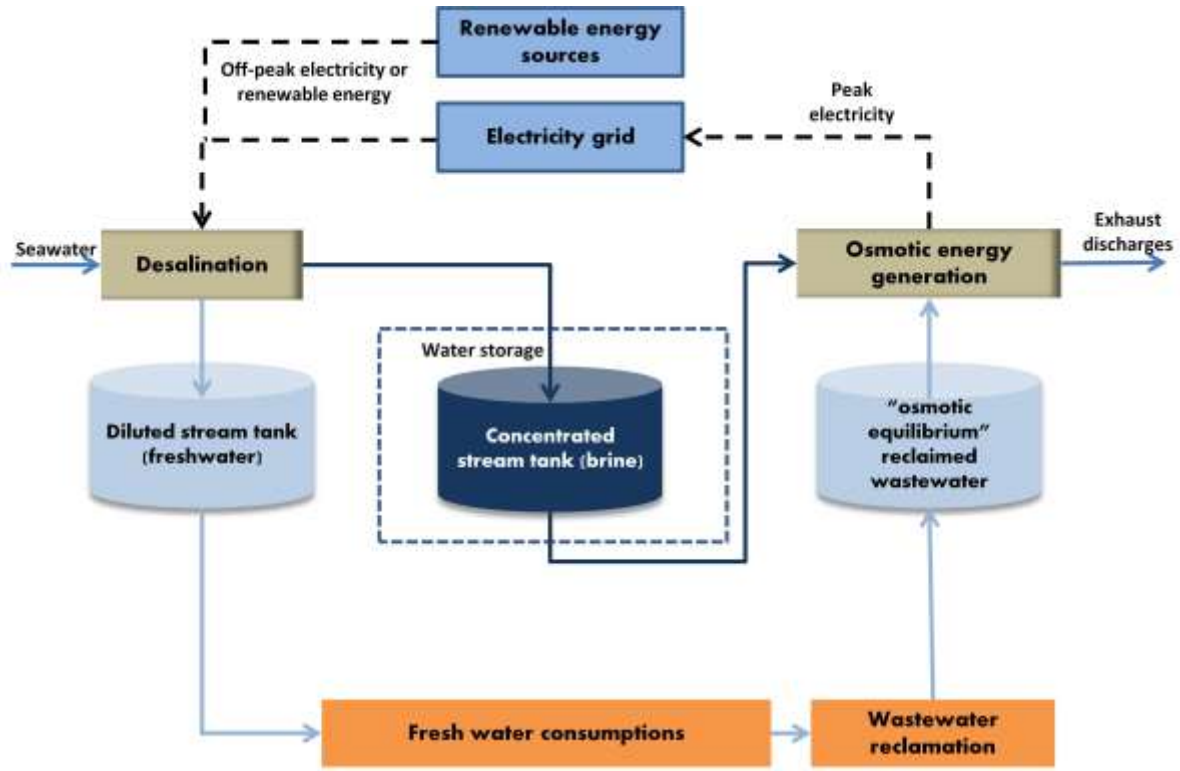

Figure 4 An illustration of CWES coupled with freshwater production.

4. Case study of CWES using RO and PRO

In this section, the proposed CWES using RO and PRO is analysed and the cycle efficiency of the energy storage is evaluated by simulation. Without the consideration of the membrane fouling, the thermodynamic analysis of the proposed CWES using "osmotic-equivalent" reclaimed wastewater is almost identical to the CWES as shown in Fig. 3 due to the same initial conditions and configuration. Therefore, both the CWES systems are analysed thermodynamically in this section. At first, to explore the limiting performance of a CWES using RO and PRO, the energy losses caused in pressurization and expansion are not considered, namely efficiencies of 100% are assumed for all machines. Inefficiency of these component will be discussed later. Furthermore, from the previous studies, it is observed that the insignificant effect of density variation on the solutions obtained in the range of salinity studied

[53, 54], for simplicity, a constant density of the water, 1,000 kg/m^3, is used for all the concentrations considered in this work.

4.1. Mathematical models

Mathematical models of RO have been widely studied in the last several decades and the models of the scale-up PRO process have been also extensively studied in recent years [11, 55, 56]. In this study, two different models describing the RO and PRO are used, including the models with the ideal mass transfer and the models with performance limiting effects such as concentration polarization (CP). First, the models describing the ideal performance of these two membrane processes without considering CP effects are introduced.

Energy consumption of BP is not considered in this study for simplicity as it is negligible compared to that consumed by HP. According to the RO desalination system illustrated in Fig. 3, the minimum energy consumption in the desalination during the charge time can be represented as,

$$E_{charge}^{RO} = \Delta P^{RO} V_S^{RO} - \Delta P^{RO} V_B^{RO} = \Delta P^{RO} V_P^{RO} \tag{5}$$

where V_S^{RO}, V_B^{RO} and V_P^{RO} are volumetric flow rates of the seawater, brine and permeate in the RO desalination, respectively. ΔP^{RO} is the applied pressure.

In the absence of a pressure drop in the RO membrane module, with the high permeable membrane, the minimum required pressure should be very close to the osmotic pressure of the RO concentrate at the membrane outlet, which is called thermodynamic restriction of cross-flow RO desalinating [33]. Therefore, if the membrane is assumed to be fully rejection of salts, the lower bound of the applied pressure is,

$$\Delta P_{\min}^{RO} = \frac{\pi_S}{1-Y} \tag{6}$$

where π_S is the osmotic pressure of the initial saline stream.

For an ideal PRO process, ignoring effects of CP and RSP, when a constant pressure ΔP^{PRO} is applied on the draw solution, the work generated without considering the energy losses caused by the machines can be expressed as,

$$E_{discharge}^{PRO} = \Delta P^{PRO} \Delta V_P^{PRO} \tag{7}$$

where ΔP^{PRO} is the pressure applied on the draw solution and ΔV_P^{PRO} is the volumetric flow rate of the permeation across the membrane in the PRO sub-system. For a single-stage PRO osmotic energy generator as shown in Fig. 3, according to the work carried out by Yip et al. [51], the maximum work extracted from the stored water streams can be obtained,

$$\begin{aligned}
\Delta P_{\max}^{PRO} &= \nu RT[(1-Y)c_B^{RO} - Yc_P^{RO} + (2Y-1)\sqrt{c_B^{RO} c_P^{RO}}] \\
\Delta V_{P,\max}^{PRO} &= \frac{\sqrt{c_B^{RO}} - \sqrt{c_P^{RO}}}{\sqrt{c_B^{RO}} + \frac{Y}{1-Y}\sqrt{c_P^{RO}}} V_P^{RO} \\
E_{discahrge,\max}^{PRO} &= \Delta P_{\max}^{PRO} \Delta V_{P,\max}^{PRO} = \nu RT(1-Y)(\sqrt{c_B^{RO}} - \sqrt{c_P^{RO}})^2 V_P^{RO}
\end{aligned} \tag{8}$$

where $\Delta P_{\max}^{PRO}$, $\Delta V_{P,\max}^{PRO}$ and $E_{discharge,\max}^{PRO}$ are optimum pressure, permeation flow rates and the maximum extractable work, respectively.

4.2. Cycle efficiency of CWES using RO and PRO

The cycle efficiency of the energy storage, also called round-trip efficiency, is a key parameter to describe the performance of the "pure energy storage system" in which the energy input is solely electricity. The ratio of energy put in to energy retrieved from storage can be presented by,

$$\eta = \frac{E_{discharge}}{E_{charge}} \tag{9}$$

where $E_{discharge}$ and E_{charge} are energy released in discharge period and energy used in charge period, respectively.

In the CWES, for single-stage RO, the minimum work required to separate the water from a saline stream is obtained when the applied pressure equals to the osmotic pressure of the brine at the exit. The minimum energy used in the desalination sub-system during the charge can be represented by equation (5) and substituting the minimum applied pressure of the RO which is operated at the thermodynamic restriction. Additionally, in the single-stage PRO osmotic energy generator, the maximum extractable work of mixing the brine and freshwater from the RO desalination can be estimated based on equation (7). The energy conversions of these processes are illustrated in Fig. 5. In Fig. 5(a), to meet the RO water recovery 0.5, an applied pressure close to 60 bar is needed to make sure the non-zero water flux through the entire membrane module for full-scale water permeation. As a consequence, the minimum work required can be represented by the rectangular area in the left side of Fig. 5(a). After the separation in the RO, the initial condition of the PRO is based on the brine and freshwater resulted from the RO. Therefore, the osmotic pressure difference at the beginning of the PRO is equal to that at the end of the RO. Also, in order to maintain the non-zero flux through the entire membrane module and harvest the maximum energy by a single-stage PRO generator, a pressure close to 30 bar is needed to apply on the brine. Similarly, the maximum extractable work from a single-stage PRO can be represented by the rectangular at the right side of Fig. 5(a). Therefore, the limiting cycle efficiency of the CWES with single-stage RO and single-stage PRO is the area ratio of the right rectangular to the left one in the Fig. 5(a).

Furthermore, when the water recovery of the RO varies, the performance of the entire CWES is changed accordingly. As illustrated in Fig. 5(a), when the water recovery is 0.3, on one hand, the minimum work required to separate the water from the seawater is significantly reduced compared to that with RO water recovery 0.5. On the other hand, as shown in Fig. 5(b), the energy generated by the PRO also decreases due to the reduced energy density of the stored water bodies. As a result, the cycle efficiencies are also changed. Four operating conditions of the CWES are evaluated and listed in Table 1 in which both the cycle efficiency and the energy density are selected as the overall performance of the entire energy storage system.

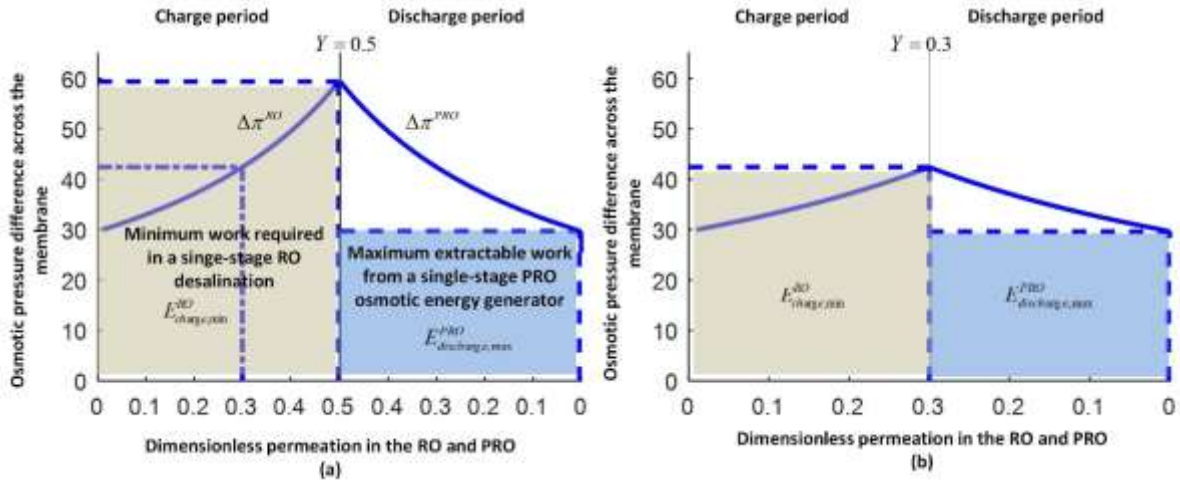

Figure 5 Illustration of the minimum required work in a single-stage RO process, the maximum work extracted from a single-stage PRO process, and maximum cycle efficiency of the CWES using the single-stage RO and the single-satge PRO. In (a), the water recovery ratio of the RO is 0.5. In (b), the water recovery ratio is 0.3.

According to the results shown in Table 1, the cycle efficiency with the RO water recovery 0.3 is larger than that with the RO water recovery 0.5, when the initial RO feed is seawater with 35 g/L concentration. The result is due to the nature of the ratio of the cycle efficiency. As illustrated in Fig. 5(b), although both the energy consumption in the RO and the energy generated in the PRO are reduced, the fraction to be harnessed from the stored water bodies increases indicating the increased effectiveness of the single-stage PRO osmotic energy generator at the low RO water recovery.

Moreover, the maximum cycle efficiency is significantly affected by the water recovery ratio in the RO desalination sub-system rather than the concentration of the initial saline stream. As shown in Table 1, with different concentrations of the initial salinity, namely 35 g/L and 70 g/L, the cycle efficiencies are quite close when the water recovery ratios are same. In fact, due to the concentration of the brine is considerably larger than that of the permeate in the RO desalination, consequently, the cycle efficiency can be further approximated by,

$$\eta_{\max} = \frac{\Delta P_{\max}^{PRO} \Delta V_{P,\max}^{PRO}}{\Delta P_{\min}^{RO} V_{P,\min}^{RO}} \approx \frac{\nu RT(1-Y)\left(\sqrt{\frac{c_S}{1-Y}}\right)^2 V_P^{RO}}{\nu RT \frac{c_S}{1-Y} V_P^{RO}} = 1-Y \tag{10}$$

Therefore, the approximated limiting cycle efficiency of the CWES using the RO and PRO is inversely proportional to the water recovery ratio in the desalination. With higher RO water recovery, lower limiting cycle efficiency is resulted. Interestingly, it is opposite to the maximum energy density of stored waters. As shown in Fig. 2, the energy density of the stored waters increases with the increase on the water recovery. Based on the results shown in Table 1, the trader-off relationship between the cycle efficiency and the energy density can be also found. For example, in the section of the overall performance of the CWES, energy density of the stored water increases significantly from 0.2939 Wh/L to 0.5712 Wh/L, when the water recovery ratio increase from 0.3 to 0.5 using the seawater (35 g/L) as the initial RO feed. Same trend is obtained in the cases using 70 g/L as the initial RO feed that the energy density increases from 0.5879 Wh/L to 1.1426 Wh/L. In contrast, the cycle efficiencies of the both initial salinities decrease from approximately 68% to about 49%, when the RO water recovery is changed from 0.3 to 0.5, respectively.

Because of the independence of the limiting cycle efficiency on the salinities' concentration, for the balance of these trade-off objectives, it is recommended to use a solution with higher concentration as the initial RO feed and operate the CWES at a lower RO water recovery. At such operation, the CWES is expected to have high cycle efficiency and an acceptable energy density.

Table 1 Several cases study of the CWES using the RO and PRO with two initial salinities and two RO water recoveries.

Salinity concentration available				
Concentration of the available solution, g/L	35	70	35	70
RO desalination sub-system				
Water recovery, V_P^{RO} / V_S^{RO}	0.3	0.3	0.5	0.5
Optimum applied pressure, bar	42.40	84.79	59.35	118.71
Minimum work required during charge period, kWh per 1 m^3 initial feed solution to RO	0.3533	0.7066	0.8243	1.6487
PRO osmotic energy generator sub-system				
Dimensionless permeation rate, $\Delta V_P^{PRO} / V_P^{RO}$	0.980	0.986	0.976	0.983
Optimum applied pressure, bar	29.43	59.01	29.67	59.35
Maximum released energy during discharge period, kWh per 1 m^3 initial feed solution to RO	0.2404	0.4848	0.4024	0.8105
Overall performance of the CWES				
Maximum cycle efficiency, $E_{discharge,\max}^{PRO} / E_{charge,\min}^{RO}$	68.03%	68.61%	48.81%*	49.16%
Stored energy density, Wh/L	0.2939	0.5879	0.5712	1.1426

4.3. Effects of concentration polarization and salt leakage on cycle efficiency

The analysis above are based on the ideal mass transfer model of both the RO and PRO processes in which the flows have homogeneous concentration and membranes are fully rejected for the salts. For the RO membrane, on the basis of the well-developed membrane fabrication and the mature technology of the RO desalination, vary high performance of the RO membrane and process are available in practice [48]. However, at the early stage of developing specific PRO membrane, the detrimental effects of the mass transfer need to be considered. Actually, CP or/and salt leakage are major detrimental effects in the realistic operations, which significantly affect the overall performance of the membrane processes. Therefore, the effects of the CP and salt leakage are considered and evaluated by simulation in this section.

To predict the realistic performance of the RO and PRO processes, in recent years, several mathematical models have been developed and verified with the experimental data. In this study, the selected previously validated models of the RO and PRO considering these detrimental effects from literatures are listed in Table 2 and 3, respectively. In the RO modelling, the ECP on the RO feed side is considered. In contrast, in the PRO modelling, ICP inside of the support layer, ECP next to the active layer and the RSP across the membrane are considered. The details of these mathematical models can be found in [48] and [55], respectively. Parameters selected from the literatures are used, which are shown in Table 4.

Table 2 Mathematical model of the RO desalination from [48].

Mathematical model of the RO desalination sub-system	
Water flux	$J_{W,RO} = A^{RO}(\Delta P^{RO} - \Delta\pi) = A^{RO}(\Delta P^{RO} - C_{OS}(c_{B,m} - c_{P,m}))$

Effect of CP	$c_{B,m} = c_{B,b}\exp(\frac{J_{W,RO}}{k})$
Water permeation	$d(\Delta q_P) = J_{w,RO}d(A_{m,RO})$
Concentration of the brine	$c_{B,\mathrm{b}} = \frac{\mathrm{c}_S^0 q_S^0}{q_B}$
Flow rate of the brine	$q_B = q_S^0 + \Delta q_P$
Flow rate of the permeate	$q_P = \Delta q_P$

*symbols used in Table 1 can be found in Nomenclature.

TABLE 3 Mathematical model of the PRO osmotic energy generator from [55].

Mathematical model of the PRO osmotic energy generator sub-system	
Water flux	$J_{W,PRO} = A^{PRO}(\Delta P^{RO} - \Delta P) = A^{PRO}(C_{OS}(c_{D,m} - c_{F,m}) - \Delta P)$
Effects of CP and RSP	$c_{D,m} - c_{F,m} = \frac{c_{D,b}\exp(-J_{W,PRO}/k) - c_{\mathrm{F,b}}\exp(J_{W,PRO}S/D)}{1 + \frac{B}{J_{W,PRO}}[\exp(J_{W,PRO}S/D) - \exp(-J_{W,PRO}/k)]}$
Solute flux	$J_S = B(c_{D,m} - \mathrm{c}_{F,m})$
Water permeation	$d(\Delta V_P) = J_{w,PRO}d(A_{m,PRO}); \Delta q_P = \rho_P \Delta V_P$
Salt permeation	$d(\Delta V_S) = J_S d(A_{m,PRO}); \Delta m_S = \rho_S \Delta V_S$
Concentration of the draw	$c_{D,\mathrm{b}} = \frac{\mathrm{c}_D^0 q_D^0 - \Delta m_S}{q_D}$
Concentration of the feed	$c_{F,b} = \frac{\mathrm{c}_\mathrm{F}^0 q_F^0 + \Delta m_S}{q_F}$
Flow rate of the draw	$q_D = q_D^0 + \Delta q_P$
Flow rate of the feed	$q_F = q_F^0 - \Delta q_P$

*symbols used in Table 2 can be found in Nomenclature.

TABLE 4 Parameters used in the simulation to evaluate the effects of CP in both the RO and PRO and RSP in the PRO.

RO desalination sub-system parameters [48]	
Membrane water permeability coefficient, $\mathrm{L\cdot m^{-2}\cdot h^{-1}\cdot bar^{-1}}$	1.3
Membrane rejection	100%
Mass transfer coefficient, $\mathrm{m\cdot s^{-1}}$	3×10^{-5}
PRO osmotic energy generator sub-system parameters [55]	
Membrane water permeability coefficient, $\mathrm{L\cdot m^{-2}\cdot h^{-1}\cdot bar^{-1}}$	1.74
Membrane salt permeability coefficient, $\mathrm{L\cdot m^{-2}\cdot h^{-1}}$	0.16
Membrane structural parameter, μm	307
Mass transfer coefficient, $\mathrm{L\cdot m^{-2}\cdot h^{-1}}$	3.85×10^{-5}
Diffusion coefficient, $\mathrm{m^2\cdot s^{-1}}$	1.49×10^{-9}

The effect of the ECP in the RO desalination system is shown in Fig. 6(a). Because of the high salt rejection of the membrane which is reasonably assumed to be 100% due to the current commercial RO membranes [48], the scale of the permeation from the RO feed in the separation is not changed under a particular applied hydraulic pressure. As shown in Fig. 6(a), with the increased membrane area, the osmotic pressure difference approaches to the same value of the ideal PRO process, although

the ECP results in larger membrane area which causes reduction of the RO membrane effectiveness. However, based on the energy consumption of the RO operated at the thermodynamic restriction, the ECP effect does not affect the minimum work required to meet the pre-defined water recovery ratio if the enough membrane is available.

Similar to the ECP effect in the RO desalination, the CP effects also reduce the membrane effectiveness in the osmotic energy generator. Moreover, due to the lack of the high performance of the specific PRO membrane, the maximum work extracted by the single-stage PRO process is reduced. The salt leakage from the high concentration side to the low concentration side, accelerate the concentration process of the low concentration solution and the dilution process of the concentrated solution and terminate the energy conversion before meeting the final mixed concentration of the ideal mixing. As a consequence, only part of the theoretical chemical potential between the stored salinities is harnessed by the PRO according to the reduced scale of permeation. As shown in Fig. 6(b), the practical work extracted is only fraction of the theoretical maximum work of the single-stage PRO. The other part of the theoretical maximum extractable energy is lost due to the un-extracted mixing energy of accumulating RSP across the membrane.

Therefore, excluding the reduction on the membrane effectiveness in both membrane processes, the overall performance of the CWES is also changed due to the reduced osmotic energy generation during the discharge period. In fact, the optimum pressure to achieve the maximum osmotic energy generation is also varied with respect to the effects of the CP and RSP [57]. Thus, the same four operating conditions of the CWES are evaluated considering the CP and ECP in the PRO osmotic energy generator. The results are shown in Table 5. All the cycle efficiencies are decreased due to the CP and RSP effects in the PRO. The maximum efficiency of the CWES with RO water recovery 0.3 is less than 55% and the cycle efficiency of the system with RO water recovery 0.5 reduced to less than 42%.

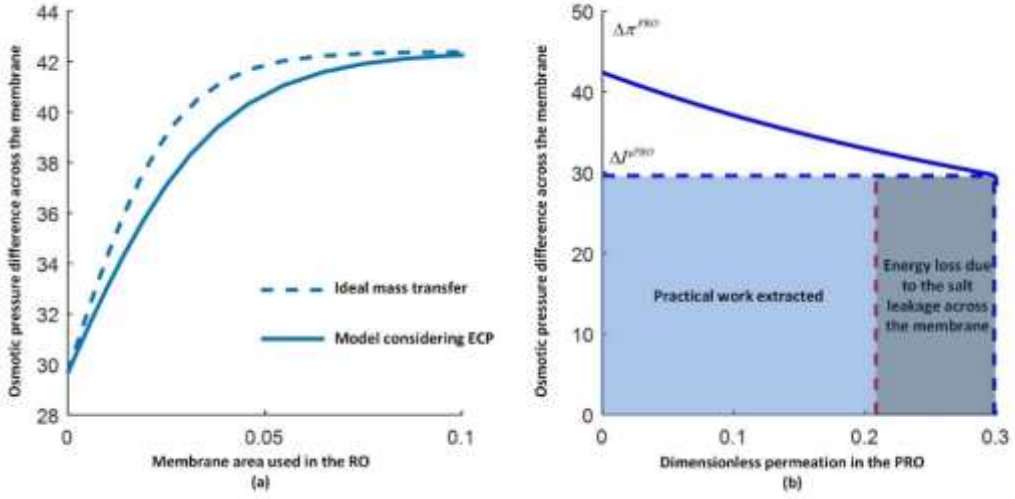

Figure 6 Effects of the CP and RSP in the CWES using the RO and PRO. In (a), the ECP effect in the RO desalination is considered. In (b), the ICP, ECP and RSP effects are considered in the PRO osmotic energy generator.

Table 5 Varied performance of the CWES due to the CP and RSP in the PRO osmotic energy generator sub-system.

	Salinity concentration available			
Concentration of the available solution, g/L	35	70	35	70
RO desalination sub-system				

Water recovery, V_P^{RO} / V_S^{RO}	0.3	0.3	0.5	0.5
PRO osmotic energy generator sub-system				
Dimensionless permeation rate, $\Delta V_P^{PRO} / V_P^{RO}$	0.8678	0.8812	0.8460	0.8657
Optimum applied pressure, bar	25.7	52.9	27.8	56.4
Maximum released energy during discharge period, kWh per 1 m^3 initial feed solution to RO	0.1859	0.3885	0.3267	0.6782
Overall performance of the CWES				
Maximum cycle efficiency, $E_{discharge,\max}^{PRO} / E_{charge,\min}^{RO}$	52.61%	54.98%	39.63%*	41.13%

452

453 4.4. Energy losses in CWES

454 There is no free lunch apparently that irreversibility occurs at each conversion through the whole
455 CWES. From separation during the charge period to the osmotic energy generation during the
456 discharge period, energy losses at different levels are accompanied. First, because of constant
457 pressure operation in both single-stage RO and single-stage PRO processes, as shown in Fig. 5, more
458 energy consumed during the charge and less energy released during the discharge due to the entropy
459 generation. The deviations between the constant pressure operation represented by the rectangular
460 areas and the reversible operation lead to the exergy decrease of the saline stream and energy losses
461 increase. This irreversibility caused by single-stage configuration can be improved by implementing
462 multi-stage RO or/and multi-stage PRO to reduce the unnecessary exergy losses and drive the
463 operation close to the reversible operation. In addition, because of the detrimental effects during the
464 mass transfer, especially for osmotic energy generation using PRO, energy losses are significant due
465 to the reverse salt leakage. This portion of energy losses is caused by the performance of the
466 membrane, which can be improved by the continuously development of high-performance membrane
467 fabrication. According to a recent study, the prototype PRO plant has shown the promising results of
468 both membrane performance and resulted energy generation at the system level [45]. These
469 improvements on the membrane performance will help the CWES toward the expected cycle
470 efficiency listed in Table 1.

471 Moreover, energy losses in the pressurisation and de-pressurisation due to the inefficiencies of
472 the HP and HT also affect the overall round trip efficiency of a CWES. A set of efficiencies are selected
473 to illustrate their effects on the cycle efficiency and the results considering both detrimental effects
474 and components' inefficiencies are listed in Table 6. The efficiencies of HP, ERD and HP selected in the
475 estimations are 90%, 98% and 90% respectively and two salinities with water recovery 0.3 are
476 simulated. As indicated in Table 6, cycle efficiency of CWES becomes lower compared to those listed
477 in Table 5 due to energy losses in pressurising and expanding water. But with the future improvements
478 on the design, operation and control of these machines, higher efficiency could be expected and cycle
479 efficiency will be improved.

480

481 **Table 6** Estimated cycle efficiency of CWES considering detrimental effect in mass transfer and energy losses due to
482 inefficiencies of HP, ERD and HT.

Efficiencies of HP, ERD and HT	90%, 98% and 90%	
Concentration of the available solution, g/L	35	70
Water recovery, V_P^{RO} / V_S^{RO}	0.3	0.3
Maximum cycle efficiency, $E_{discharge,\max}^{PRO} / E_{charge,\min}^{RO}$	40.71%	42.55%

4.5. Economic cost

Furthermore, it is difficult to estimate the cost for a prototype CWES. A set of preliminary cost analysis is performed by taking advantages of the experiences gained from RO and PRO plants. A concept of added electricity cost due to energy storage is used in the estimation to the cost of CWES. It is similar to the method used by Poonpun et al, who presented a cost analysis of grid-connected electric energy storage through life cycle analysis [58]. They compared the costs of technologies including PHS, flywheels, and battery units of lead acid (LA), valve-regulated LA, sodium sulfur (Na/S), zinc/bromine (Zn/Br) and vanadium redox (VB) [58]. According to their study, the battery storage system which is 8 hours charge/discharge cycle per day adds \$0.18-0.64 per kWh to the cost of electricity and the added cost of PHS is about \$0.05 per kWh [58].

From the literature, empirical cost correlations of the RO and PRO plant are found for estimation of the prototype CWES plant. Choi et al. performed a completed economic evaluation of 100,000 m^3/day RO desalination plant including capital and operating costs of the intake, pre-treatment, HP, BP, RO membrane module, and ERD [59]. They correlated relationship between produced water cost and electricity cost in RO [59], which is

$$C_{RO} = 4.32C_E + 0.28 \tag{11}$$

where C_E is electricity cost in \$/kWh, and C_{RO} is water cost of RO system in \$ per 1 m^3 permeation from RO system.

In addition, Loeb proposed a preliminary economic correlation of the production of energy from concentrated streams by PRO. The contributions to the developed unit cost of energy includes amortisation, membrane replacement, pre-treatment and costs of labours, diversion dam and attendant piping [60]. The overall costs of the salinity energy is estimated to be,

$$C_{PRO} = (\frac{0.0036}{J} + 0.01)f + 0.004 \tag{12}$$

where J is permeation flux in $m^3/(m^2 \cdot day)$, f is the permeation/energy ratio of PRO in m^3/kWh.

It needs to note that these cost correlations of both RO and PRO systems are dependent on many factors, such as the system design/scales, membrane costs and etc. Although these costs are application-dependent, these economic analysis can be regarded as “ballpark” estimation and useful to indicate the possible cost of CWES. Therefore, the added electricity price due to CWES can be estimated

$$\Delta C = C_{RO}\frac{f}{f_P} + C_{PRO} - C_E \tag{13}$$

where $f_P = \Delta V_P^{PRO} / V_P^{RO}$ is permeation/feed ratio of PRO system, and ΔC is the added electricity cost in \$/kWh. Furthermore, if parts of the produced freshwater from the RO system are sold with water price, C_W, the added electricity cost can be written as

$$\Delta C = (C_{RO} - C_W f_W)\frac{f}{f_P} + C_{PRO} - C_E \tag{14}$$

where f_W is the percentage of the sold freshwater.

The added electricity cost due to CWES operated in the four operations as shown in Table 5 are plotted in Fig. 7 in which operation (a) is salinity concentration 35 g/L, water recovery 0.3; operation (b) is salinity concentration 70 g/L, water recovery 0.3; operation (c) is salinity concentration 35 g/L,

water recovery 0.5; and operation (d) is salinity concentration 70 g/L water recovery 0.5. According to the results, CWES without selling freshwater shows relatively similar added electricity cost compared to the results of batteries in [58]. Considering the off-peak electricity price which is less than £0.9/kWh in the UK (~$1.2/kWh), the added electricity costs of operations (a) and (c) are in the range of $0.45 - $1.19 per KWh; and those of operations (b) and (d) are in the range of $0.22 - $ 0.51 per KWh. Moreover, if parts of freshwater from RO system are sold at water price $1/m^3 [61], the added electricity cost due to CWES can be significantly reduced. Therefore, the economic viability of the proposed CWES is achieved only the added electricity cost is less than the difference of the price between the peak and off-peak times. As an energy storage technology, the proposed CWES offers the flexibility in managing the profits by selling both the produced freshwater and electricity.

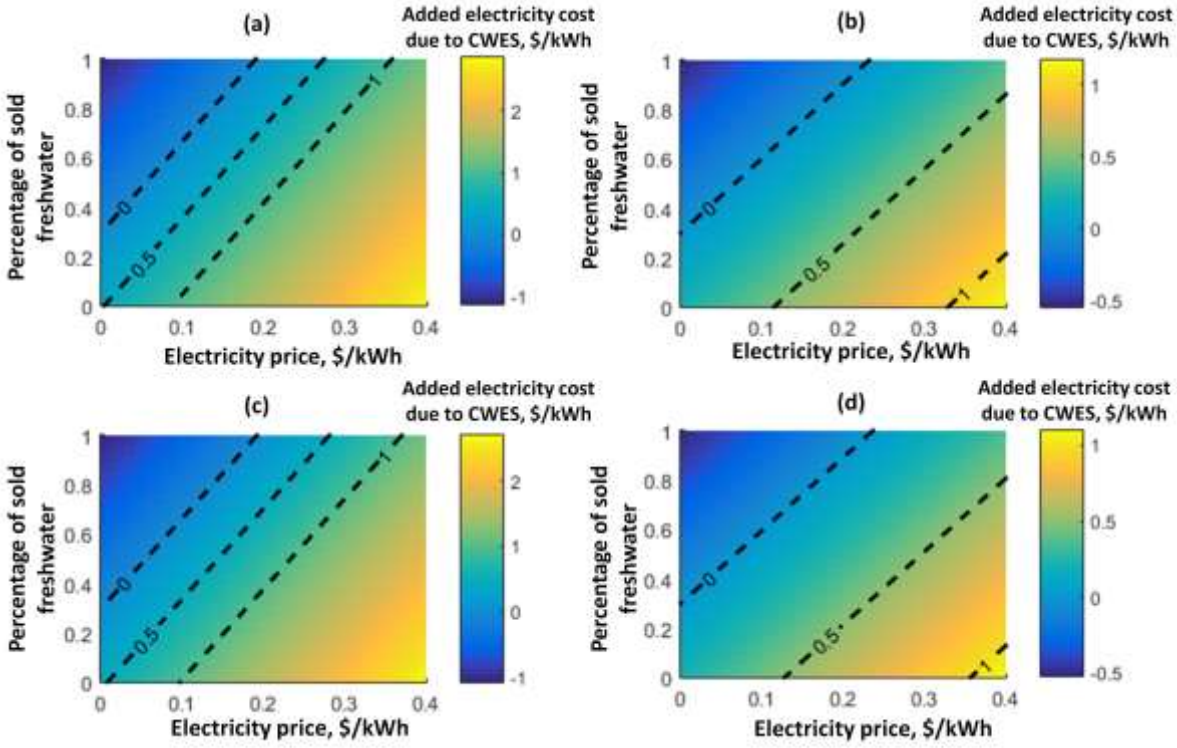

Figure 7 Added electricity cost due to CWES operated in the four operations as shown in Table 5.

5. Conclusion

A preliminary study on the feasibility of the energy storage by concentrating/desalinating water is carried out in the proposed CWES system. The work first introduces the proposed configuration and operation of a generic CWES system and evaluated the energy density of the stored waters. Then, several scenarios of the CWES are proposed and a systematic analysis of the CWES using RO and PRO is developed with respect to different operations. Based on the results, several conclusions can be drawn: 1) energy density of a generic CWES depends on the initial saline concentration. In the range of defined water recovery 0 to 0.8, using seawater (35 g/L) as the initial saline stream, energy density is more than 1.5 Wh/L and using brine (70 g/L) as the initial saline stream, energy density is more than 2.5 Wh/L. 2) a dual purposes of energy storage and freshwater production is achieved by a CWES using "osmotic-equivalent" wastewater. 3) limiting cycle efficiency of the CWES using single-stage RO and single-stage PRO is inversely proportional to the RO water recovery and independent on the concentration of the initial salinity. 4) trade-off relationship of the cycle efficiency and energy density

is found. In order to meet satisfactory values of both the objectives, a higher concentration of the initial saline solution can be used as the initial saline stream in the CWES using RO and PRO and the CWES needs to be operated at a lower RO water recovery. 5) Detrimental effects during the mass transfer in the PRO reduces the osmotic energy generation and the cycle efficiency of the CWES. 6) CWES potentially offers a flexibility of operation to meet economic viability.

Acknowledgement

Thanks to the funding support from Engineering and Physical Science Research Council (EPSRC), UK (EP/L014211/1 and EP/K002228/1). The authors also want to thank the support from China 973 Research Programme (2015CB251301) to enable the discussion with Chinese partners.

Nomenclature

Symbol

G	Gibbs free energy, J
c	Concentration, g/kg
q	Mass flow rate, kg/s
x	Mole fraction, mol/mol
R	Gas constant, $J \cdot K^{-1} \cdot kg^{-1}$
T	Temperature, K
γ	Activity coefficient
ϕ	Ratio of moles of two solutions
ν	Van't Hoff factor, $bar \cdot kg \cdot g^{-1}$
Y	Water recovery ratio
V	Volume flow rate, $m^3 \cdot s^{-1}$
P	Pressure, Pa
E	Energy, J
π	Osmotic pressure, Pa
η	Cycle efficiency
J_w	Water flux, $L \cdot m^{-2} \cdot h^{-1}$
A	Membrane water permeability coefficient, $L \cdot m^{-2} \cdot h^{-1} \cdot bar^{-1}$
A_m	Membrane area, m^2
B	Membrane salt permeability coefficient, $L \cdot m^{-2} \cdot h^{-1}$
k	Mass transfer coefficient, $L \cdot m^{-2} \cdot h^{-1}$

582	D	Diffusion coefficient, $m^2 \cdot s^{-1}$
583	C_{OS}	Modified van't Hoff coefficient, $bar \cdot kg \cdot g^{-1}$
584	S	Membrane structure parameter, m
585	C	Unit economic cost, $/unit
586		
587	*Subscript/superscript*	
588	*mix* , *M*	Mixing
589	*i*	Specie of salt
590	*high*	Solution with high concentration
591	*low*	Solution with low concentration
592	*s*	Initial saline stream
593	*B*	Brine
594	*P*	Permeation
595	*ch*arg*e*	Operation of charging period
596	*disch*arg*e*	Operation of discharging period
597	*RO*	Reverse osmosis
598	*PRO*	Pressure retarded osmosis
599	min	Minimum
600	max	Maximum
601		
602	*Acronym*	
603	CWES	Concentrated water energy storage
604	PHS	Pumped hydroelectric storage
605	CAES	Compressed air energy storage
606	RO	Reverse osmosis
607	PRO	Pressure retarded osmosis
608	MSF	Multi-stage flash
609	MED	Multi-effect distillation
610	TVC	Thermal vapour compression
611	AD	Adsorption desalination
612	MD	Membrane distillation

FO	Forward osmosis
HDH	Humidification-dehumidification
ED	Electrodialysis
MVC	Mechanical vapour compression
CDI	Capacitive deionization
RED	Reverse electrodialysis
CAPMIX	Capacitive mixing

Appendix: Maximum energy densities of pumped hydro-energy storage (PHS) and compressed air energy storage (CAES)

A.1 Pumped hydro-energy storage (PHS)

PHS is the most widely used large scale electrical energy storage in the world at the moment. PHS represents more than 99% of worldwide bulk storage capacity and contributes to about 3% of global generation [62]. It requires very specific site condition to make the plant viable, such as high head, favourable topography, good geotechnical conditions, access to electricity transmission networks and water availability [63]. Among these criteria, the most influential factor to determine the energy density is available site with a satisfactory elevation difference and access to water. According to the comprehensive review carried out by Deane et al, the head of current PHS plants worldwide is in the range of 100-800 m [63]. One of the world's largest ultra-high head (~779 m) large capacity plant is Kazunogawa PHS in Japan [63]. The theoretical energy density of a PHS with the basics of gravitational potential energy can be presented as,

$$e_{PHS} = \frac{mgH}{V} \tag{A.1}$$

where e_{PHS} is maximum energy density of a PHS with head H . g is gravitational acceleration rate, m is mass flow rate and V is volume flow rate.

A.2 Compressed air energy storage (CAES)

In addition to PHS, another larger scale electrical energy storage (over 100 MW) is CAES. In a conventional CAES, air is compressed using surplus electricity during the period of low power demand, and is expanded to generate electricity during the period of high power demand.

On the basis of the different CAES systems, the pressure of the compressed air in the storage varies. Generally, the maximum energy of compressed air in cavern can be evaluated using the second law of thermodynamics. If the compressed air storage is assumed to be operated isothermally, the maximum exergy stored of compressed air with pressure P_1 and T_1 in a cavern with volume V can be estimated

$$e_{CAES} = \frac{m_1}{V} R T_0 \ln(P_1 / P_0) \tag{A.2}$$

where T_0 is ambient temperature, P_0 is atmosphere pressure, m_1 is mass of air in cavern when air pressure is P_1. Based on ideal gas theory, equation (A.2) can be further written as

$$e_{CAES} = P_1 \ln(P_1 / P_0) \quad \text{(A.3)}$$

Reference:

[1] Sternberg A, Bardow A. Power-to-What? - Environmental assessment of energy storage systems. Energy & Environmental Science. 2015;8:389-400.

[2] REN21. Renewables 2015: global status report. acessed in 18/09/2015, <http://www.ren21.net/wp-content/uploads/2015/07/GSR2015_KeyFindings_lowres.pdf> 2015.

[3] Chen H, Cong TN, Yang W, Tan C, Li Y, Ding Y. Progress in electrical energy storage system: A critical review. Progress in Natural Science. 2009;19:291-312.

[4] van der Linden S. Bulk energy storage potential in the USA, current developments and future prospects. Energy. 2006;31:3446-57.

[5] Segurado R, Madeira JFA, Costa M, Duić N, Carvalho MG. Optimization of a wind powered desalination and pumped hydro storage system. Applied Energy. 2016;177:487-99.

[6] Stenzel P, Linssen J. Concept and potential of pumped hydro storage in federal waterways. Applied Energy. 2016;162:486-93.

[7] Luo X, Wang J, Krupke C, Wang Y, Sheng Y, Li J, et al. Modelling study, efficiency analysis and optimisation of large-scale Adiabatic Compressed Air Energy Storage systems with low-temperature thermal storage. Applied Energy. 2016;162:589-600.

[8] Wathen A. Preconditioning and convergence in the right norm. International Journal of Computer Mathematics. 2007;84:1199-209.

[9] Rastler D. Electricity Energy Storage Technology Options: A White Paper Primer on Applications. Costs and Benefits, EPR Institute, Palo Alto, CA. 2010.

[10] Luo X, Wang J, Dooner M, Clarke J. Overview of current development in electrical energy storage technologies and the application potential in power system operation. Applied Energy. 2015;137:511-36.

[11] Jiménez Capilla JA, Carrión JA, Alameda-Hernandez E. Optimal site selection for upper reservoirs in pump-back systems, using geographical information systems and multicriteria analysis. Renewable Energy. 2016;86:429-40.

[12] Zakeri B, Syri S. Electrical energy storage systems: A comparative life cycle cost analysis. Renewable and Sustainable Energy Reviews. 2015;42:569-96.

[13] The future role for energy storage in the UK main report. Energy Research Partnership (ERP) technology report. Accessed in 18/09/2015, <http://erpuk.org/wp-content/uploads/2014/10/52990-ERP-Energy-Storage-Report-v3.pdf>. 2011.

[14] Saadat M, Shirazi FA, Li PY. Modeling and control of an open accumulator Compressed Air Energy Storage (CAES) system for wind turbines. Applied Energy. 2015;137:603-16.

[15] Ghaffour N, Missimer TM, Amy GL. Technical review and evaluation of the economics of water desalination: Current and future challenges for better water supply sustainability. Desalination. 2013;309:197-207.

[16] Logan BE, Elimelech M. Membrane-based processes for sustainable power generation using water. Nature. 2012;488:313-9.

[17] Anastasio DD, Arena JT, Cole EA, McCutcheon JR. Impact of temperature on power density in closed-loop pressure retarded osmosis for grid storage. Journal of Membrane Science. 2015;479:240-5.

[18] McGinnis R, Mandell A. Utility scale osmotic grid storage. Google Patents; 2014.

[19] Shaulsky E, Boo C, Lin S, Elimelech M. Membrane-Based Osmotic Heat Engine with Organic Solvent for Enhanced Power Generation from Low-Grade Heat. Environmental Science & Technology. 2015;49:5820-7.
[20] Reimund KK, McCutcheon JR, Wilson AD. Thermodynamic analysis of energy density in pressure retarded osmosis: The impact of solution volumes and costs. Journal of Membrane Science. 2015;487:240-8.
[21] Gude VG. Desalination and sustainability – An appraisal and current perspective. Water Research. 2016;89:87-106.
[22] Bennett A. 50th Anniversary: Desalination: 50 years of progress. Filtration + Separation. 2013;50:32-9.
[23] Bennett A. Advances in desalination energy recovery. World Pumps. 2015;2015:30-4.
[24] Li Y-L, Tung K-L, Chen Y-S, Hwang K-J. CFD analysis of the initial stages of particle deposition in spiral-wound membrane modules. Desalination. 2012;287:200-8.
[25] Borsani R, Rebagliati S. Fundamentals and costing of MSF desalination plants and comparison with other technologies. Desalination. 2005;182:29-37.
[26] Lattemann S, Höpner T. Environmental impact and impact assessment of seawater desalination. Desalination. 2008;220:1-15.
[27] Sharaf MA, Nafey AS, García-Rodríguez L. Thermo-economic analysis of solar thermal power cycles assisted MED-VC (multi effect distillation-vapor compression) desalination processes. Energy. 2011;36:2753-64.
[28] Ng KC, Thu K, Kim Y, Chakraborty A, Amy G. Adsorption desalination: An emerging low-cost thermal desalination method. Desalination. 2013;308:161-79.
[29] Alkhudhiri A, Darwish N, Hilal N. Membrane distillation: A comprehensive review. Desalination. 2012;287:2-18.
[30] McGinnis RL, Elimelech M. Energy requirements of ammonia–carbon dioxide forward osmosis desalination. Desalination. 2007;207:370-82.
[31] Narayan GP, Lienhard JH. Humidification Dehumidification Desalination. Desalination: John Wiley & Sons, Inc.; 2014. p. 425-72.
[32] Ghaffour N, Bundschuh J, Mahmoudi H, Goosen MFA. Renewable energy-driven desalination technologies: A comprehensive review on challenges and potential applications of integrated systems. Desalination. 2015;356:94-114.
[33] Zhu A, Christofides PD, Cohen Y. Effect of Thermodynamic Restriction on Energy Cost Optimization of RO Membrane Water Desalination. Industrial & Engineering Chemistry Research. 2009;48:6010-21.
[34] Sadrzadeh M, Mohammadi T. Sea water desalination using electrodialysis. Desalination. 2008;221:440-7.
[35] Aly NH, El-Figi AK. Mechanical vapor compression desalination systems — A case study. Desalination. 2003;158:143-50.
[36] Oren Y. Capacitive deionization (CDI) for desalination and water treatment — past, present and future (a review). Desalination. 2008;228:10-29.
[37] Awerbuch L. Future Directions in Integration of Desalination, Energy and the Environment. http://web.mit.edu/ans/www/documents/seminar/S09/awerbuch_slides.pdf>. accessed in 15.09.2015. 2009.
[38] Achilli A, Childress AE. Pressure retarded osmosis: From the vision of Sidney Loeb to the first prototype installation — Review. Desalination. 2010;261:205-11.
[39] Veerman J, Saakes M, Metz SJ, Harmsen GJ. Reverse electrodialysis: Performance of a stack with 50 cells on the mixing of sea and river water. Journal of Membrane Science. 2009;327:136-44.
[40] Brogioli D. Extracting renewable energy from a salinity difference using a capacitor. Physical review letters. 2009;103:058501.
[41] Porto RL, Frappier R, Ducros JB, Aucher C, Mosqueda H, Chenu S, et al. Titanium and vanadium oxynitride powders as pseudo-capacitive materials for electrochemical capacitors. Electrochimica Acta. 2012;82:257-62.

[42] Jia Z, Wang B, Song S, Fan Y. Blue energy: Current technologies for sustainable power generation from water salinity gradient. Renewable and Sustainable Energy Reviews. 2014;31:91-100.
[43] He W, Wang Y, Shaheed MH. Maximum power point tracking (MPPT) of a scale-up pressure retarded osmosis (PRO) osmotic power plant. Applied Energy. 2015;158:584-96.
[44] Kurihara M, Hanakawa M. Mega-ton Water System: Japanese national research and development project on seawater desalination and wastewater reclamation. Desalination. 2013;308:131-7.
[45] Sakai H, Ueyama T, Irie M, Matsuyama K, Tanioka A, Saito K, et al. Energy recovery by PRO in sea water desalination plant. Desalination.
[46] Gerstandt K, Peinemann KV, Skilhagen SE, Thorsen T, Holt T. Membrane processes in energy supply for an osmotic power plant. Desalination. 2008;224:64-70.
[47] MVP G. Global leader of next generation desalination "Creat Water, Lead the Future". <http://www.globalmvp.org/english/sub/project/plant.htm> accessed in 15.09.2015.
[48] Banchik LD, Sharqawy MH, Lienhard V JH. Effectiveness-mass transfer units (ε-MTU) model of a reverse osmosis membrane mass exchanger. Journal of Membrane Science. 2014;458:189-98.
[49] Beaudin M, Zareipour H, Schellenberglabe A, Rosehart W. Energy storage for mitigating the variability of renewable electricity sources: An updated review. Energy for Sustainable Development. 2010;14:302-14.
[50] Díaz-González F, Sumper A, Gomis-Bellmunt O, Villafáfila-Robles R. A review of energy storage technologies for wind power applications. Renewable and Sustainable Energy Reviews. 2012;16:2154-71.
[51] Yip NY, Elimelech M. Thermodynamic and Energy Efficiency Analysis of Power Generation from Natural Salinity Gradients by Pressure Retarded Osmosis. Environmental Science & Technology. 2012;46:5230-9.
[52] Lin S, Straub AP, Elimelech M. Thermodynamic limits of extractable energy by pressure retarded osmosis. Energy & Environmental Science. 2014;7:2706-14.
[53] Wiley DE, Fletcher DF. Techniques for computational fluid dynamics modelling of flow in membrane channels. Journal of Membrane Science. 2003;211:127-37.
[54] Fletcher D, Wiley D. A computational fluids dynamics study of buoyancy effects in reverse osmosis. Journal of membrane science. 2004;245:175-81.
[55] He W, Wang Y, Shaheed MH. Modelling of osmotic energy from natural salt gradients due to pressure retarded osmosis: Effects of detrimental factors and flow schemes. Journal of Membrane Science. 2014;471:247-57.
[56] He W, Wang Y, Shaheed MH. Energy and thermodynamic analysis of power generation using a natural salinity gradient based pressure retarded osmosis process. Desalination. 2014;350:86-94.
[57] Banchik LD, Sharqawy MH, Lienhard V JH. Limits of power production due to finite membrane area in pressure retarded osmosis. Journal of Membrane Science. 2014;468:81-9.
[58] Poonpun P, Jewell WT. Analysis of the cost per kilowatt hour to store electricity. IEEE Transactions on energy conversion. 2008;23:529-34.
[59] Choi Y, Shin Y, Cho H, Jang Y, Hwang T-M, Lee S. Economic evaluation of the reverse osmosis and pressure retarded osmosis hybrid desalination process. Desalination and Water Treatment. 2016:1-12.
[60] Loeb S. Production of energy from concentrated brines by pressure-retarded osmosis. Journal of Membrane Science. 1976;1:49-63.
[61] Villafafila A, Mujtaba IM. Fresh water by reverse osmosis based desalination: simulation and optimisation. Desalination. 2003;155:1-13.
[62] Electrical energy storage: white paper. Technical report. Prepared by electrical energy storage project team. <http://www.iec.ch/whitepaper/pdf/iecWP-energystorage-LR-en.pdf>. 2011.
[63] Deane JP, Ó Gallachóir BP, McKeogh EJ. Techno-economic review of existing and new pumped hydro energy storage plant. Renewable and Sustainable Energy Reviews. 2010;14:1293-302.